Integrated PSO-MILP water–energy planning and operation under flexibility constraints and water scarcity: Application to an off-grid Mediterranean island

Utilities Policy 101 (2026) 102219

Contents lists available at ScienceDirect

Utilities Policy

journal homepage: www.elsevier.com/locate/jup

Full-length article

Integrated PSO-MILP water–energy planning and operation under flexibility constraints and water scarcity: Application to an off-grid Mediterranean island

Matteo Savina [a], Carlo Federico Vescovo [b,1], Giovanni Zaccaria [e], Enrico Giglio [c,d,*], Giuliana Mattiazzo [c,d]

[a] Department of Mathematical Sciences, Politecnico di Torino, Corso Duca degli Abruzzi 24, 10129, Torino, Italy
[b] Department of Computer Science, College of Engineering, University of Illinois Chicago, 850 W Taylor St, 60607, Chicago, IL, USA
[c] Department of Mechanical and Aerospace Engineering, Politecnico di Torino, Corso Duca degli Abruzzi 24, 10129, Torino, Italy
[d] Marine Offshore Renewable Energy Lab (MOREnergy Lab), Politecnico di Torino, Via Paolo Borsellino 38/16, 10138, Torino, Italy
[e] Department of Automation and Computer Engineering, Politecnico di Torino, Corso Duca degli Abruzzi 24, 10129, Torino, Italy

ARTICLE INFO

Handling Editor: Janice A. Beecher

Keywords:
Water–energy nexus
MILP energy planning
PSO
PyPSA
Non-interconnected islands
Desalination
Flexibility

ABSTRACT

Rising water demand and global energy transition represent two of the most pressing systemic challenges. Where freshwater is scarce, supply increasingly depends on electricity-intensive desalination, while power systems themselves are undergoing rapid transformation driven by the growing penetration of variable renewable energy sources. Both dynamics impose a major need for flexibility: desalination adds large, inflexible loads, and variable renewables amplify operational uncertainty. Although often treated separately, these issues are deeply interconnected—both at the planning and operational levels. This work introduces a hybrid PSO-MILP framework that jointly optimizes long-term investment and short-term operation in coupled power and water systems. The model explicitly accounts for desalination flexibility, hydrogen production and storage, unit commitment, and downward reserve requirements. By linking water demand and availability with power dispatch and reserve provision, desalination is modeled as a demand-side management resource, effectively substituting for conventional storage and enabling higher renewable penetration. The framework is demonstrated on Pantelleria, a non-interconnected Mediterranean island. Results show that enabling reserve provision from clean technologies such as batteries and desalination plants reduces total system costs by nearly 47% and raises the renewable share from 41% to 87%. Flexible desalination scheduling further cuts costs by up to 30%. Even when freshwater demand doubles, renewable penetration falls only 6%, with modest increases in offshore wind capacity. These findings confirm the strategic relevance of integrated planning in water-constrained energy systems.

1. Introduction

1.1. Motivation

Meeting the growing global water demand is a critical challenge, especially in regions with limited freshwater availability (Rosa and Sangiorgio, 2025). Desalination has emerged as a reliable solution, yet its high energy consumption remains a barrier to widespread and sustainable adoption (Almasoudi and Jamoussi, 2024). This issue is particularly acute on small islands, where desalination units are often powered by fossil fuel generators (FFGs) (Palmeros Parada et al., 2023). To reduce emissions and enhance sustainability, renewable energy sources (RES) offer a promising alternative. In particular, variable RES (vRES) such as solar and wind are well-suited for island environments due to high potential availability (Stunjek and Krajačić, 2025). However, both desalination and vRES pose operational challenges: the high energy demand of desalination (Esquivel-Puentes et al., 2025) and the intermittency of vRES (Brijs et al., 2017) can each destabilize isolated grids by causing sudden power imbalances and frequency deviations (Giorcelli et al., 2025). Addressing these issues requires clean

* Corresponding author.
E-mail addresses: matteo.savina@polito.it (M. Savina), cvesc@uic.edu (C.F. Vescovo), giovanni.zaccaria@studenti.polito.it (G. Zaccaria), enrico.giglio@polito.it (E. Giglio), giuliana.mattiazzo@polito.it (G. Mattiazzo).
[1] The work was initiated while Carlo Federico Vescovo was a research fellow at the Department of Law, Universitá di Torino, Turin, Italy.

https://doi.org/10.1016/j.jup.2026.102219
Received 4 September 2025; Received in revised form 20 April 2026; Accepted 23 April 2026
Available online 29 April 2026

Acronyms

FFG	Fuel-fired generator
VRES	Variable renewable energy sources
PV	Photovoltaic units
FOWT	Floating Offshore Wind Turbines
BESS	Battery energy storage systems
DES	Desalination plants
ELY	Electrolyzer
FC	Fuel cell

Indices and Sets

g	Indices of Fuel-fired generator (FFG) unit
r	Indices of vRES generation unit
s	Indices of storage units
d	Indices of desalination units
e	Indices of electrolyzers
a	Indices of a generic technology ($a \in \{g, r, s, d\}$)
t	Indices of operating snapshots $t = 1, \ldots, t_{end}$
l	Index of electrical load node
ln	Index of transmission lines
Ω_G	Set of FFGs
Ω_R	Set of vRES generation techs
Ω_S	Set of storages
Ω_D	Set of desalinators
Ω_L	Set of loads
Ω_A	Set of all technologies
Ω_{LN}	Set of electrical network lines

Parameters

cc	capital costs
oc	operational costs
f_{obj}	objective function
CC_{tot}	Total capital cost
OC_{tot}	Total operational cost
$sw(t)$	Weight of the tth snapshot
$K_{ln,n}$	networks' incident matrix in the line ln-th of the nth node
η_s^{ch}	charging efficiency coefficients
η_s^{disch}	discharging efficiency coefficients
η_s^{sd}	self-discharge coefficient
$CF_r(t)$	capacity factor of rth VRES unit
$d_s^{ch}(t)$	mean hourly charge power of the sth battery
$d_s^{disch}(t)$	mean hourly discharge power of the sth storage unit
$e_{max,s}$	maximum SoC of the sth storage unit
$e_{min,s}$	minimum SoC of the sth storage unit
$P_{nom,a}$	Nominal capacity (power) of the ath technology
$P_{mod,a}$	Nominal capacity (power) of a single unit of the ath technology
$n_{mod,a}$	Number of modules installed for a technology a
$E_{nom,s}$	Nominal capacity of the sth storage unit.
$d_a(t)$	Mean hourly electrical power supplied or procured at tth time step by the ath unit.
$e_s(t)$	State-of-Charge of the sth storage at tth timestep.
$p_{max,s}^{disch}$	Maximum percentage of safe discharge power of the sth store unit
$p_{max,s}^{ch}$	Maximum percentage of safe charge power of the sth store unit
$p_{min,a}(t)$	Min percentage of power that can be supplied or procured by the ath technology at tth timestep.
$p_{max,a}(t)$	Max percentage of power that can be supplied or procured by the ath technology at tth timestep.
$s_a(t)$	Status (on/off) of the ath component at tth time step
$s_s^{ch}(t)$	Status (on/off) of the charging link of the sth storage technology
$s_s^{disch}(t)$	Status (on/off) of the discharging link of the sth storage technology
$dw(t)$	Water demand at tth time step.
$dw_f(t)$	Residential water demand at tth time step.
$dw_{H_2}(t)$	Water demand for hydrogen production at tth time step.
α_w	Stand-by energy consumption coefficient, constant for all desalination units
β_w	specific energy consumption (SEC) per unit of time, constant for all desalination units of each desalinator
α_e	stand-by energy consumption coefficient, constant for all desalination units
β_e	specific energy consumption (SEC) per unit of time, constant for all desalination units of each desalinator
T_{mu}^d	minimum turn-on time steps
$r_a(t)$	down reserve of the ath component at tth time step
$R_{rq}(t)$	down reserve requirement at tth time step
ε_{fix}	fix term of the hourly reserve request
$l_l(t)$	Electrical load at node l and time t
$f_{ln}(t)$	Power flow on line ln at time t
$EL(t)$	Electric load at tth time step
w_{EL}	Weight of electric load in the computation of the reserve requirements
w_r	Weight of VRES in the computation of the reserve requirements
$P_r(t)$	Expressed VRES power at tth snapshot
$I(t)$	Water tank level
I_{max}	Maximum capacity of the water tank
$w_d(t)$	Water produced by the dth desalination unit

technologies capable of providing flexibility, both in terms of load management and power reserve (Babatunde et al., 2020). Desalination units and storage systems, if properly coordinated, can contribute to power system stability while meeting water demand (Giglio et al., 2025a). This calls for integrated energy planning that evaluates long-term sizing decisions against short-term operational constraints in coupled water–power systems, including flexible desalination scheduling and reserve management. Moreover, among storage technologies, hydrogen (H2) offers seasonal storage (Go et al., 2023). However, its production via electrolysis significantly increases both water and energy demands, especially in freshwater-scarce environments (Simoes et al., 2021). This reinforces the need to tightly couple water and energy systems, particularly when the deployment of storage technologies depends on desalinated water.

Lastly, jointly optimizing the planning and operational aspects of energy and water systems may introduce non-linearities (Giglio et al., 2025c)—particularly due to the coupling between desalination scheduling, H2 production, and power reserve management—which make the problem intractable with standard Mixed-Integer Linear Programming (MILP) approaches. A possible solution lies in the use of integrated frameworks that combine water system management, desalination, and H2 technologies within energy planning models, while addressing system flexibility and non-linear dynamics through hybrid MILP–Particle

Table 1
Classification of studies by flexible Water Demand, long-term planning, UC, costs, reserves, desalination, and H_2 integration.

Study	Island	Flexible WD	Planning	UC	Opex	Reserve	Desalinator	H_2
Al-Mubarak and Conejo (2025)		✓	✓		✓	✓	✓	
Elbalki et al. (2024)		✓	✓		✓	✓	✓	
Wen et al. (2024)		✓	✓			✓	✓	✓
Groppi et al. (2023)	✓	✓	✓		✓	✓		✓
Stunjek and Krajačić (2025)	✓	✓	✓		✓		✓	
Arunachalam et al. (2024)						✓	✓	✓
Liu et al. (2023)		✓		✓	✓	✓	✓	✓
Guo et al. (2021)		✓		✓	✓		✓	
Astolfi et al. (2017)	✓	✓		✓	✓	✓		
Elsir et al. (2022)		✓		✓	✓	✓		
Oikonomou and Parvania (2019)		✓		✓	✓	✓	✓	
Alnahhal et al. (2023)		✓			✓	✓	✓	✓
Corsini et al. (2009)	✓	✓			✓	✓	✓	✓
Segurado et al. (2011)	✓	✓			✓	✓	✓	
Abdelsalam et al. (2024)		✓			✓	✓	✓	✓
This	✓	✓	✓	✓	✓	✓	✓	✓

Swarm Optimization (PSO)-based strategies. To the best of the authors' knowledge, such comprehensive and integrated approaches remain unexplored in the current literature.

1.2. Paper positioning

In the literature several efforts have been made to decarbonize small islands by integrating RES into local energy systems (Blechinger et al., 2016; Meschede et al., 2022). Most contributions focus on minimizing operational costs while incorporating vRES, often in combination with desalination technologies (Alnahhal et al., 2023; Corsini et al., 2009). However, these works generally neglect long-term planning aspects, which are essential when investment decisions and future system flexibility need to be addressed (Segurado et al., 2011; Abdelsalam et al., 2024).

Other studies adopt a more comprehensive approach by integrating long-term capacity expansion planning with operational optimization (Al-Mubarak and Conejo, 2025; Wen et al., 2024). In some cases, these models explore a limited set of energy planning scenarios without fully endogenizing investment decisions (Arunachalam et al., 2024; Elbalki et al., 2024). Despite their broader scope, these contributions typically omit unit commitment (UC) modeling (Stunjek and Krajačić, 2025; Groppi et al., 2023), which has proven critical to accurately estimating dispatchable generation needs and system flexibility under vRES uncertainty (Giglio et al., 2025c).

A third group of works includes UC formulations to capture short-term operational constraints and generator dynamics (Liu et al., 2023; Guo et al., 2021). While these models provide more realistic dispatch patterns, they rarely include explicit reserve requirements (Astolfi et al., 2017; Elsir et al., 2022; Oikonomou and Parvania, 2019). Reserve provision is either neglected or indirectly represented through heuristics such as renewable curtailment minimization or battery smoothing. Only a limited number of contributions jointly address long-term planning, operational cost optimization, UC, and reserve modeling (Giglio et al., 2023), yet they do not consider integrated water–energy planning.

To highlight these gaps, Table 1 presents a classification of relevant studies based on whether they include long-term planning, UC, operational costs, reserve provision, desalination, and H2 integration. As the table shows, existing contributions typically fail to simultaneously account for all these dimensions—especially in the context of small islands, where system flexibility, water availability, and seasonal storage are strongly interdependent.

To the best of the authors' knowledge, no existing study offers an integrated optimization framework that simultaneously captures all key dimensions of the water–energy nexus (Helerea et al., 2023; Vakilifard et al., 2018). In particular, the literature lacks a unified model that brings together energy planning and advanced operational modeling—such as UC and derived cost components like standby costs—while also explicitly representing the role of desalination and H2 production. In most of the previously cited works, desalination units are treated as flexible demands, but are rarely integrated into the dispatch problem with associated operational constraints and costs, such as unit-commitment formulation, capturing stand-by costs and minimum up/down-time constraints. Moreover, in scenarios involving long-term energy storage technologies that consume water—such as H2 production via electrolysis—the water demand is often ignored or decoupled from the desalination system. This omission prevents a realistic assessment of the water–energy interdependencies and may lead to suboptimal or infeasible planning outcomes, especially in water-scarce environments like non-interconnected islands (Mehrjerdi, 2020a).

1.3. Contributions and structure of the work

This work introduces a unified optimization framework for isolated water–energy systems, jointly optimizing long-term planning and short-term operations. The model explicitly captures the interplay between energy dispatch, desalination, and H2 production, while incorporating reserve requirements and key operational constraints. A hybrid PSO-MILP strategy is employed to effectively address the coupling between planning and operational optimization in the integrated water–energy nexus. The framework has been implemented in an open-source environment and made available to the scientific community (Giglio et al., 2025d). Its application is demonstrated on the non-interconnected Mediterranean island of Pantelleria, a real-world case characterized by limited freshwater resources and high renewable energy potential, yet currently reliant exclusively on diesel generation.

The remainder of this paper is structured as follows. Section 2 details the proposed PSO-MILP optimization framework, describing both the planning and operational layers and their integration. Section 3 introduces the Pantelleria case study and defines the scenario settings. Section 4 outlines the optimization process and discusses computational performance, while Section 5 presents and analyzes the results of the planning and dispatch optimization under different water demand and reserve settings. Finally, Section 6 concludes the work and identifies areas for future research.

2. Methodology: A PSO-MILP framework for integrated water–energy nexus planning and operation

This section presents the methodological framework developed to optimize the design and operation of isolated water–energy systems. The model integrates long-term capacity expansion and short-term operational scheduling, capturing the complex interactions between renewable generation, reserve provision, desalination, and H2 production. Although the problem could in principle be formulated in different ways, in the most widespread implementations (Giglio et al., 2025c)—particularly those available in open-source frameworks (i.e. PyPSA (Brown et al., 2018))—it is characterized as a Mixed-Integer Nonlinear Programming (MINLP) model due to the presence of bilinear terms, which will be further discussed in Section 2.2. These couplings make the problem computationally challenging and difficult to solve directly. To overcome these challenges, a hybrid optimization approach is adopted—combining MILP with PSO. This PSO-MILP framework enables the simultaneous exploration of high-level system designs and detailed operational decisions while enforcing technical constraints and maintaining computational tractability. The methodology is organized in two interconnected layers:

- **PSO-based planning layer.** This layer of the model searches the design space by varying the number of installed units per technology (e.g., photovoltaic - PV, wind turbines - WT, Battery energy storage systems - BESS, desalinators -DES, electrolyzers - ELY, fuel cell - FC). This modularity-based approach allows for discrete capacity expansion decisions while capturing the combinatorial nature of the investment space.
- **MILP-based operational model.** This component optimizes the system's operational variables given a fixed energy–water planning configuration provided by the PSO layer. It includes energy balances and advanced operational constraints based on a UC formulation, such as power reserve requirements and energy–water coupling. Specifically, the coupling between the energy and water systems is modeled through the explicit representation of the energy demand associated with desalination—linked to the quantity of water produced—and H2 production, where both electricity and water consumption are considered. The MILP formulation determines optimal dispatch schedules and computes the total system cost for each candidate planning configuration.

The overall structure of the proposed hybrid framework, and the interaction between the PSO-based planning and MILP-based operational layers, is illustrated in Fig. 1.

2.1. Water–energy nexus planning through PSO

PSO is a population-based metaheuristic inspired by the collective behavior observed in natural swarms, such as bird flocks or fish schools (Kennedy and Eberhart, 1995; Jain et al., 2022). It is particularly well suited for the global exploration of complex, non-convex design spaces (Abdi et al., 2013; Gad, 2022). It has also recently become popular for addressing optimization problems in energy systems scenarios (EL-Qasery et al., 2025; Esmaeilion et al., 2025). In the proposed framework, PSO is employed to determine the optimal sizing of key infrastructure components using a modular approach, where each technology—PV, WT, BESS, DES, ELY—is composed of discrete installable units. The decision variables specify the number of units to install for each technology. Each particle in the swarm represents a candidate system configuration, encoded as an integer vector as in Eq. (1). Within the position vector, each component $n_i \in \mathbb{N}$ corresponds to the number of units associated with a specific technology.

$$\mathbf{x} = \left[n_{\mathrm{PV}}, n_{\mathrm{WT}}, n_{\mathrm{BESS}}, n_{\mathrm{DES}}, n_{\mathrm{ELY}}, n_{\mathrm{FC}}\right] \tag{1}$$

Particle positions evolve over time based on velocity updates that incorporate individual memory and social influence. The velocity at iteration $t+1$ is controlled by Eq. (2), where $v_i^{(t)}$ is the current velocity of particle i, p_i^{best} is its personal best position, and g^{best} is the global best found by the swarm. The parameters w, c_1, and c_2 govern inertia, self-confidence, and social learning, respectively. Random variables r_1 and r_2, drawn from a uniform distribution over $[0, 1]$, introduce exploratory variability. Using the updated velocity, the new position of each particle is computed as shown in Eq. (3), which defines the candidate configuration for the next iteration. Since the decision variables represent discrete quantities, each component of $x_i^{(t+1)}$ is rounded to the nearest integer and constrained within technology-specific bounds that reflect feasible installation limits.

$$v_i^{(t+1)} = w v_i^{(t)} + c_1 r_1 \left(p_i^{\mathrm{best}} - x_i^{(t)}\right) + c_2 r_2 \left(g^{\mathrm{best}} - x_i^{(t)}\right), \tag{2}$$

$$x_i^{(t+1)} = x_i^{(t)} + v_i^{(t+1)}. \tag{3}$$

The fitness of each particle is the total annual energy system cost which is computed by solving the MILP operational model associated with the proposed configuration (see Eq. (4), introduced below in Section 2.2.1). As the swarm iterates, it converges toward infrastructure setups that effectively balance investment and performance. PSO therefore functions as a global search mechanism well suited for modular system design in discrete and nonlinear contexts.

2.2. MILP framework for optimizing water–energy nexus operation

The adopted MILP framework models the operational behavior and cost structure of a power microgrid, while also capturing key operational features of the water system—such as reservoir availability and freshwater demand dynamics. Special attention is given to the coupling between the two sectors, with a particular focus on the operational flexibility introduced by desalination, which is represented within a set of techno-economic constraints. Specifically, the microgrid includes diesel generators, RES (PV and WT), BESS with associated transformers, DES, and ELY equipped with tanks and fuel cells. DES and ELY have a direct impact on the water subsystem, which also includes a freshwater reservoir. The two hourly load profiles considered as fixed inputs to the model are the electricity demand and the freshwater demand curve, both defined exogenously. The section is structured as follows: first, the objective function of the MILP water–energy optimization model is presented; then, for each subsystem, the governing equations are introduced to describe their operational behavior and reserve contributions.

2.2.1. Objective function

The objective function (4) minimizes the total system cost, which includes both capital expenditures (CAPEX) and operational expenditures (OPEX). The PSO searches for the configuration that minimizes the total system cost, while the MILP only ensures that for every configuration, the resulting OPEX is minimal. Capital costs, shown in Eq. (5), are computed as the sum of non-recurring investment costs for all subsystems, including FFGs, vRES technologies, storage systems with associated converters, desalination, and H2 components. Operational costs, defined in Eq. (6), represent recurring expenditures such as fuel consumption and maintenance for generation and storage assets.

$$\min f_{\mathrm{obj}} = \min(CC_{\mathrm{tot}} + OC_{\mathrm{tot}}) \tag{4}$$

$$CC_{\mathrm{tot}} = \sum_{g=1}^{\Omega_G} cc_g P_{\mathrm{nom},g} + \sum_{r=1}^{\Omega_R} cc_r P_{\mathrm{nom},r} + \sum_{s=1}^{\Omega_S} \left(cc_s E_{\mathrm{nom},s} + cc_{s,\mathrm{links}} P_{\mathrm{nom},s}\right) + \sum_{d=1}^{\Omega_D} cc_d P_{\mathrm{nom},d} \tag{5}$$

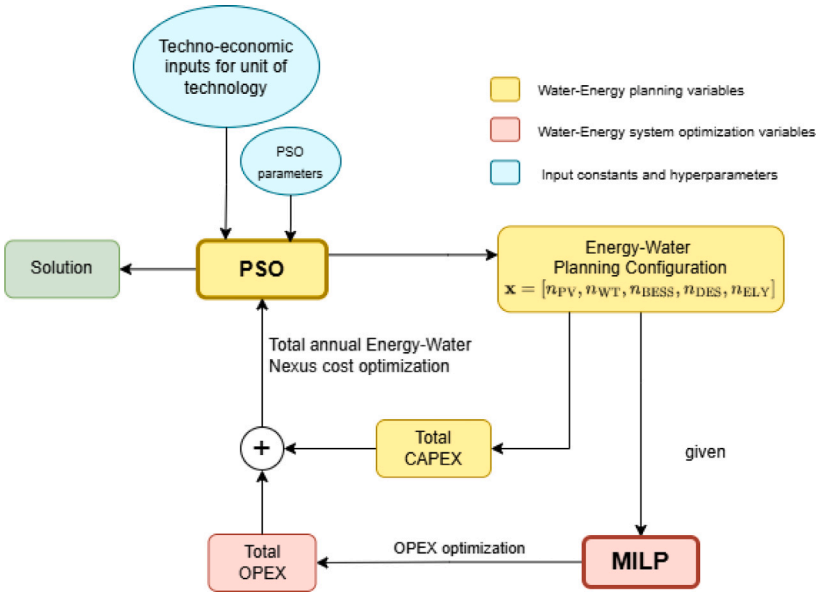

Fig. 1. Optimization flow for energy–water planning using PSO-MILP framework.

$$OC_{\mathrm{tot}} = \sum_{t=1}^{t_{\mathrm{end}}} sw(t) \left(\sum_{g=1}^{\Omega_G} oc_g d_g(t) + \sum_{s=1}^{\Omega_S} oc_s d_s(t) + \sum_{d=1}^{\Omega_D} oc_d d_d(t) \right) \tag{6}$$

2.2.2. Modeling the power system

In order to ensure power system balance at each node, Eq. (7) enforces the nodal power balance constraint at every time step t. It ensures that total electricity generation and incoming power flows equal the total consumption, including charging demands, loads, and desalination requirements. In this formulation, $f_{ln,t}$ denotes the power flow in the line ln-th with networks' incident matrix $K_{ln,n}$, while η_s^{ch} and η_s^{disch} are the charging and discharging efficiency coefficients, respectively.

$$\begin{aligned} &\sum_{a \in (\Omega_G \cup \Omega_R)} d_a(t) + \sum_{s \in \Omega_S} d_s^{disch}(t) \cdot \eta_s^{disch} + \sum_{ln \in \Omega_{LN}} f_{ln}(t) \cdot K_{ln,n} \\ &= \sum_{s \in \Omega_S} \frac{d_s^{ch}(t)}{\eta_s^{ch}} + \sum_{l \in \Omega_L} l_l(t) + \sum_{d \in \Omega_D} d_d(t) \end{aligned} \tag{7}$$

Eq. (8) ensures that the power output of each dispatchable diesel generator remains within its operational limits, bounded by the minimum and maximum load factors, and is conditional on the unit's activation status $s_g(t)$. In addition, Eq. (9) models the FFGs' contribution to downward reserve provision, again conditional on their on/off status.

$$s_g(t) \cdot p_{min,g} \cdot P_{nom,g} \leq d_g(t) \leq p_{max,g} \cdot P_{nom,g}, \quad \forall g \in \Omega_G \tag{8}$$

$$r_g(t) \leq d_g(t) - p_{min,g} \cdot P_{\mathrm{nom},g}, \quad \forall g \in \Omega_G \cdot s_g(t) \tag{9}$$

The behavior of vRES is governed by the availability of the corresponding natural resource, which is captured through a time-varying capacity factor. Eq. (10) constrains the instantaneous power output of each vRES unit to the product of its nominal capacity and capacity factor at time t.

$$d_r(t) \leq P_{\mathrm{nom},r} \cdot CF_r(t), \quad \forall r \in \Omega_R \tag{10}$$

Concerning storage systems, the model includes a set of operational constraints that ensure technical feasibility and realistic battery behavior. Eq. (11) enforces that the state of charge (SoC) remains bounded between the minimum and maximum admissible energy levels, scaled by the nominal capacity of each battery system. Eq. (12) constrains the power exchanged by the storage system—whether charging or discharging—based on converter limits, which are defined as a percentage of nominal power and are conditional on the binary activation status $s_s(t)$. Finally, Eq. (13) updates the SoC dynamically at each time step, accounting for charging efficiency, discharging losses, and self-discharge.

$$E_{\mathrm{nom},s} \cdot e_{\mathrm{min},s} \leq e_s(t) \leq E_{\mathrm{nom},s} \cdot e_{\mathrm{max},s}, \quad \forall s \in \Omega_S \tag{11}$$

$$s_s(t) \cdot p_{\mathrm{min},s}(t) \cdot P_{\mathrm{nom},s} \leq d_s(t) \leq p_{\mathrm{max},s} \cdot P_{\mathrm{nom},s}, \quad \forall s \in \Omega_S \tag{12}$$

$$e_s(t) = e_s(t-1) \cdot (1 - \eta_s^{sd}) - d_s^{disch}(t) + d_s^{ch}(t) \cdot \eta_s^{ch}, \quad \forall s \in \Omega_S \tag{13}$$

In addition to their storage function, batteries can contribute to power reserve provision and are thus included—together with desalination units—among the clean technologies considered for system flexibility. This ancillary role is modeled in Eqs. (14) and (15), which impose upper bounds on the reserve provided based on both instantaneous power converter capacity and available energy. Eq. (14) limits the reserve by the headroom between the converter's rated charging power and the current operating level. Eq. (15) ensures that sufficient stored energy is available to deliver the reserve power for a minimum time, taking into account charging efficiency and the current SoC.

$$r_s(t) \leq p_{max,s}^{ch} \cdot P_{nom,s} \cdot s_s^{ch}(t) - d_s^{ch}(t) + d_s^{disch}(t), \quad \forall s \in \Omega_S \tag{14}$$

$$r_s(t) \leq \eta_s^{ch} \left(E_{\mathrm{nom},s} \cdot e_{\mathrm{max},s}(t) - e_s(t) \right), \quad \forall s \in \Omega_S \tag{15}$$

2.2.3. Modeling the water system

The water system is modeled by explicitly representing the dynamics of key components: desalination units, electrolyzer, public freshwater demand, and a centralized storage tank. These elements are interconnected through a shared water network, where resource availability and consumption are dynamically balanced. The main governing equations of the water system are provided in Eqs. (16)–(18). In particular, Eq. (16) defines the total freshwater demand $dw(t)$ as the sum of residential demand $dw_f(t)$ and the water required for H2 production by electrolyzers $dw_{H_2}(t)$, where $H_2 \in \Omega_S$. Eq. (17) models the water inventory dynamics in the freshwater tank. The inventory level $I(t)$ is updated at each time step based on the aggregated production $w_d(t)$ from all DES and the total water demand $dw(t)$. Eq. (18) enforces

the upper bound on water storage capacity. In the proposed model, water produced by all DES is assumed to be collected in a single centralized reservoir with fixed capacity (i.e., not a decision variable), as the available tank volume in the case study is oversized and does not constrain desalination flexibility.

$$dw(t) = dw_f(t) + dw_{H_2}(t) \tag{16}$$

$$I(t) = I(t-1) + \sum_{d=1}^{\Omega_D} w_d(t) - dw(t) \tag{17}$$

$$I(t) \le I_{max} \tag{18}$$

2.2.4. Modeling the water–energy coupling

This Subsection describes the set of constraints that explicitly couple the water and energy systems. The interaction occurs primarily through two components: DES and electrolyzers. DES consume electricity to produce freshwater, and their operational flexibility is leveraged to provide downward power reserve. This flexibility, however, is conditioned by the availability of storage capacity in the freshwater tank, linking the energy reserve provision to the state of the water subsystem. Conversely, electrolyzers consume both electricity and freshwater to produce H2, establishing a direct coupling between the water inventory and the energy conversion process. The mathematical formulation of these couplings is presented in the following equations.

Desalinators. Desalination units contribute to the freshwater supply, which can serve both public consumption and H2 production needs. Eq. (19) models the relationship between the power consumption of the dth desalinator and the amount of freshwater it produces. The specific energy consumption coefficient β_w links power to water output, while the standby term α_w accounts for baseline consumption when the unit is active. The binary variable $s_d(t)$ indicates the on/off operational state. The power consumption is further constrained by operational bounds, as shown in Eq. (20), which limits the power to lie within a feasible range determined by the DES's nominal capacity and minimum load factor. Finally, desalinators can provide downward power reserve, depending on their operating point. The headroom between the current power and the maximum power defines the available reserve, as captured in Eqs. (21) and (22).

$$d_d(t) = \alpha_w \cdot s_d(t) + \beta_w \cdot w_d(t) \tag{19}$$

$$s_d(t) \cdot p_{min,d}(t) \cdot P_{nom,d} \le d_d(t) \le s_d(t) \cdot P_{nom,d} \tag{20}$$

$$r_d(t) \le s_d(t) \cdot P_{nom,d} - d_d(t) \tag{21}$$

$$\sum_{d \in \Omega_D} r_d(t) \le \frac{I_{max} - \sum_{d \in \Omega_D} w_d(t) - \alpha_w}{\beta_w} \tag{22}$$

Electrolyzer water consumption. Although often neglected in the literature, the water consumption associated with H2 production may become a critical aspect in water-scarce regions where freshwater is produced via energy-intensive desalination. In the proposed model, electrolyzers consume freshwater to produce H2, thereby coupling the energy and water systems. This relationship is explicitly represented in Eq. (23), where the total freshwater demand for H2 production is a linear function of the electrolyzer power input. The term α_e represents the standby water consumption, while β_e denotes the specific water consumption per unit of electricity used.

$$dw_{H_2}(t) = \alpha_e + \beta_e \cdot d_e(t) \tag{23}$$

Lastly, electrolyzers are modeled as part of the storage set Ω_S; therefore, all operational and reserve constraints defined for energy storage in Eqs. (11)–(15) also apply to them. This unified modeling approach ensures that water availability constraints are consistently enforced across all storage technologies with water dependency.

2.2.5. Power reserve requirements

The system must maintain sufficient power reserve capacity to ensure flexibility in the presence of demand uncertainty and variable renewable generation. To this end, within the proposed optimization framework, this requirement is ensured through explicit downward reserve modeling. Despite alternative modeling choices being possible (Kaldellis et al., 2017), the focus on downward reserve is justified by the specific dynamics of high-RES island grids: conventional generators often operate near their minimum technical limits to accommodate renewable penetration, making downward flexibility the binding constraint for system stability (Giglio et al., 2025a). The total reserve requirement is expressed in Eq. (24) as a combination of three terms: a fraction of the electrical load $EL(t)$, a weighted sum of the time-varying renewable generation capacity $P_r(t)$, and a fixed baseline term ε_{fix}.

$$R_{rq}(t) = w_{EL} \cdot EL(t) + \sum_{r=1}^{\Omega_R} w_r \cdot P_r(t) + \varepsilon_{\text{fix}} \tag{24}$$

This reserve requirement must be satisfied at each time step by the aggregated downward reserve provided by all eligible subsystems—FFGs, BESS, DES and ELY—as shown in Eq. (25).

$$\sum_{g=1}^{\Omega_G} r_g(t) + \sum_{s=1}^{\Omega_S} r_s(t) + \sum_{d=1}^{\Omega_D} r_d(t) \ge R_{rq}(t) \tag{25}$$

2.3. Integration of PSO and MILP via modular capacity expansion

The integration between the PSO and MILP layers is centered on the way power system capacities are defined and optimized. The PSO layer is responsible for determining the optimal installed capacity for each technology, thus addressing the discrete nature of the capacity expansion problem. For each technology, capacity expansion is represented through a modular formulation, where the total nominal capacity is defined as the product of a fixed module size and an integer number of units to install. Specifically, for each asset a in the union set Ω_A presented in Eq. (26), the nominal capacity $P_{\text{nom, a}}$ is defined as in Eq. (27).

$$\Omega_A = \Omega_G \cup \Omega_R \cup \Omega_S \cup \Omega_D \tag{26}$$

$$P_{\text{nom, a}} = P_{\text{mod, a}} \cdot n_{\text{mod, a}} \qquad \forall a \in \Omega_A \tag{27}$$

This representation reflects the discrete and modular structure of real investment processes in infrastructure planning, where generation and conversion technologies are deployed in standardized unit sizes. Once the number of units $n_{\text{mod, a}}$ has been selected by the PSO layer, the corresponding nominal capacities are passed to the MILP layer. The MILP model then optimizes the operational scheduling and unit commitment for the fixed configuration provided. This separation allows the two layers to operate in a coordinated but computationally efficient manner: PSO explores the discrete investment space, while MILP computes the optimal operational strategy for each configuration.

Moreover, this modular strategy plays a critical computational role. In a unified optimization framework, the power dispatch $d(t)$ often depends on both the unit's nominal capacity P_{nom} and its activation status $s(t)$—as seen in constraints such as Eqs. (12) and (20). If both P_{nom} and $s(t)$ were treated as decision variables in a single optimization layer, their product would create bilinear terms, making the problem nonlinear and incompatible with standard MILP solvers. By delegating the sizing decision to the PSO layer and keeping P_{nom} fixed during the MILP stage, the model ensures that $s(t) \cdot P_{\text{nom}}$ remains a linear binary-continuous product, preserving MILP tractability.

3. Case study settings: The non interconnected isle of Pantelleria

The selected case study is the island of Pantelleria, a non-interconnected island in the Mediterranean Sea, characterized by an annual electricity demand of approximately 37 GWh, based on hourly load profiles provided by the local utility. The current generation system relies exclusively on eight diesel-fired generators, hereafter referred to as FFGs for simplicity, with a total installed capacity of 24 MW. These are distributed as follows: two units rated at 1MW, four units rated at 3MW, and two units rated at 5MW.

Despite its reliance on FFGs, the island offers significant renewable energy potential, with average annual capacity factors of 19% for PV systems and 40% for floating offshore WT (FOWT). The energy planning framework allows for capacity expansion of PV, FOWT, BESS, Power Converter (Pow. Conv.) DES, and H2-based technologies, including ELY and FC. These hydrogen assets are explicitly included to evaluate the trade-off between their potential for seasonal energy shifting and the impact of their freshwater consumption on the coupled water–energy balance. No capacity expansion is considered for the existing FFGs. Onshore WT is excluded due to environmental constraints, and the maximum installable PV capacity is limited to 15 MW (Moscoloni et al., 2022). Hourly capacity factor profiles for vRES technologies were obtained from ERA5 reanalysis data (Hersbach et al., 2020). The main techno-economic assumptions are summarized in Table 2. Operational constraints include a minimum output level of 10% for FFGs, an hourly self-discharge rate of 0.1% for BESS, and a round-trip efficiency loss of 10% for battery charging and discharging. H2 conversion processes are modeled with an ELY and FC efficiency of 65% and 51%, respectively.

DES are characterized by a minimum operating load of 10% and a minimum up-time requirement of three consecutive hours, in line with typical operational constraints reported in the literature (Mehrjerdi, 2020b; Zein et al., 2023). The total annual freshwater demand is estimated at $1.08 \cdot 10^6$ m^3, with hourly consumption ranging from 60 m^3 during off-peak periods to 350 m^3 during peak summer hours. The temporal profile of water demand is assumed to follow the same distribution as electricity demand (Mentis et al., 2016). The specific energy consumption of desalination is set at 4.5 kWh/m^3 (Mohammadi et al., 2019; Airoldi et al., 2017), while standby energy consumption is considered negligible. However, time-dependent standby costs are included: 25 €/h during weekday working hours (08:00–19:00), 50 €/h overnight (19:00–08:00), and 37.5 €/h during weekend daytime hours. A key contribution of this work lies in the integrated modeling of the water–energy nexus, with particular emphasis on water consumption and operability constraints: one notable example is the explicit coupling between freshwater usage and H2 production via electrolysis, where H2 is used as a form of long-term energy storage. In this context, a freshwater consumption of 0.17 m^3 per MWh of electricity consumed by the ELY is assumed, in line with values reported for low-temperature electrolysis processes (Grubert, 2023).

Downward reserve requirements are computed by accounting for the main sources of operational uncertainty—namely, electrical load and vRES generation—through weighting factors w_{EL} and w_r, both set to 10%. In addition, a fixed term ε_{fix} of 1 MW is included, corresponding to the rated power of the smallest dispatchable generator, to ensure minimum system flexibility across all operating conditions.

MILP energy planning optimizations were conducted with the Gurobi solver (v11.0.1) in a Ubuntu 22.04.5 LTS LXC container running on an Intel Xeon E5-2697 v4 CPU @ 2.30 GHz with 256 GB of RAM. The LXC container was allocated 40 cores and 128 GB of RAM. Each optimization scenario, covering 13 representative weeks for a full year at an hourly resolution, was configured to terminate upon reaching a 2% MIP gap or a maximum runtime of 4 h. This temporal aggregation strategy was implemented by averaging the hourly data over consecutive four-week periods. This approach significantly reduces computational time while preserving the typical seasonal dynamics and daily patterns required to effectively model storage state-of-charge cycles.

3.1. Selection of the scenarios

Based on the case study settings, three scenarios have been defined to explore the impact of key operational features and reserve allocation strategies on system planning. Each scenario, summarized in Table 3, reflects a different configuration of constraints and optimization logic. The aim is to assess, in a progressive manner, how the inclusion or exclusion of specific modeling components—such as UC, flexible freshwater demand, and reserve provision—affects the planning outcomes. This staged approach enables an isolated evaluation of each feature's contribution, ultimately leading to the formulation of a comprehensive reference scenario. The following scenario pathway is adopted:

- **Reserve-DSL-Only**. Only FFGs are allowed to provide downward reserves, while unit commitment constraints are applied to both FFGs and DES. Freshwater demand is explicitly modeled, and the dispatch of DES is co-optimized within the MILP framework. This scenario closely reflects the current operational setup of the island's power system, where flexibility is ensured almost exclusively by FFGs.
- **DES-NoOptDispatch.** FW demand is translated into a fixed equivalent electrical load, thus decoupling it from the operational scheduling of DES. As a result, desalination dispatch is not optimized but treated as an exogenous, inelastic load. This configuration represents a stylized version of the current system, where desalination units operate independently of power system needs and renewable generation patterns.
- **Full.** All relevant features of the proposed framework are included. Unit commitment is applied to both FFGs and DES, freshwater demand is flexible and co-optimized with the energy system, and all technologies are allowed to contribute to reserve provision. This serves as the most comprehensive representation of the water–energy nexus and constitutes the reference scenario for comparison.

To further investigate the interaction between water scarcity and energy planning under operational constraints, each of the three scenarios reported in Table 3 is optimized under increased freshwater demand of +50% and +100% relative to the baseline. This higher water demand induces a proportional increase in electricity load, yielding total annual electricity demand from 41 GWh (baseline, without additional water demand) to approximately 44 GWh and 47 GWh under the ×1.5 and ×2 demand scenarios, respectively.

4. Optimization outcome and computational performance

Moving to the results, the next section presents detailed outcomes of the planning and dispatch optimization for each simulated scenario. Before addressing these results, however, it is necessary to focus on the integration between the PSO and MILP layers within the proposed optimization framework. In particular, this section describes the configuration of the PSO algorithm and the optimization process adopted to identify the optimal planning and dispatch strategies. Given that each objective function evaluation requires solving a distinct large-scale MILP, special emphasis is placed on the computational aspects of the optimization procedure. The PSO parameters were set to an inertia weight $w = 0.7$, cognitive coefficient $c_1 = 2.0$, and social coefficient $c_2 = 2.7$, with a swarm of 28 particles. An early-stopping criterion was adopted: the algorithm terminates if no improvement of at least 0.1% in the global best fitness is observed over 10 consecutive iterations. This was necessary because each objective function evaluation requires solving a large-scale MILP, with a high computational cost. To mitigate this burden, two efficiency strategies were implemented:

1. **MILP solution caching.** Previously visited configurations reuse cached objective values without recomputation.

Table 2
Main cost assumptions (Giglio et al., 2023, 2025c). For FC and ELY a stack lifetime of 10 years, with 50% stack, are considered.

Technology	CapEx €/kW	OpEx €/kWy	Life y	Marginal €/MWh	Stand by cost €/h	P_{mod} MW	Source
FFG	–	–	–	426	69	1,3,5	Giglio et al. (2023)
PV	905	17	25	–	–	1	Giglio et al. (2023)
FOWT	4500	94	25	–	–	1	Giglio et al. (2023)
BESS	$300\frac{1}{h}$	$6\frac{1}{h}$	15	15	–	0.5 h	Giglio et al. (2023)
Pow.Conv.	180	18	15	–	–	0.25	Giglio et al. (2023)
H2	15	–	20	–	–	0.5 h	Giglio et al. (2025b)
FC	800	32	20	–	–	0.005	Giglio et al. (2025b)
ELY	701	21	20	–	–	0.005	Giglio et al. (2025b)
DES	9000	360	25	–	25–50	0.25	Giglio et al. (2025a)

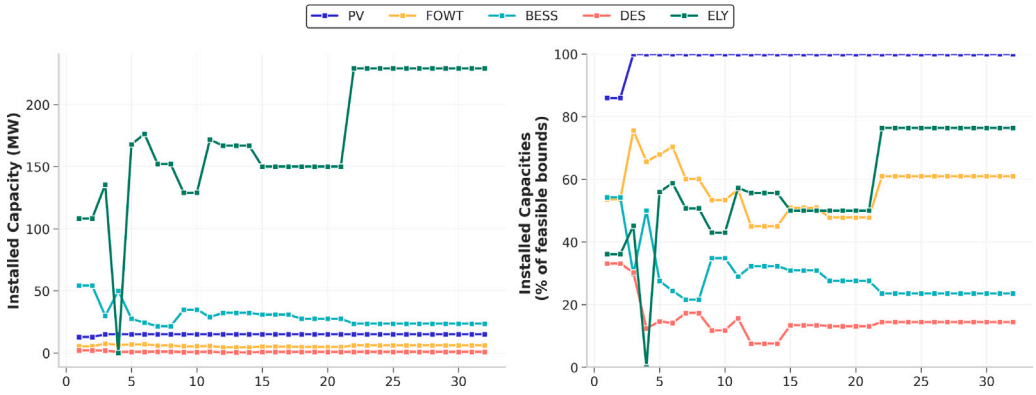

Fig. 2. Evolution of the global best across PSO iterations for the FULLx1 scenario.

Table 3
Optimized scenario configurations by operational constraints and reserve provision settings.

Scenario	Committability	Flexible Fresh Water demand	Reserveset
Reserve-DSL-Only	$\Omega_G \cup \Omega_D$	✓	Ω_G
DES-NoOptDispatch	$\Omega_G \cup \Omega_D$		Ω_A
Full	$\Omega_G \cup \Omega_D$	✓	Ω_A

2. **Lower-bound pruning.** If the MILP solver reports a lower bound greater than the particle's current best fitness, the particle evaluation is skipped.

These strategies significantly reduced overall runtimes, with a mean computational time of approximately 13 h per scenario.

Without loss of generality, since the behavior observed in the other scenarios was similar, only the FULLx1 scenario is reported. In this case the PSO achieved a mean time of 22 min per successful fitness improvement, with a standard deviation of 44 min. Out of 883 total MILP problems evaluated, 193 yielded improvements, while 690 were classified as non-promising (discarded via lower-bound pruning). The high standard deviation arises from heterogeneous evaluation times: particles exploring new configurations require full MILP resolutions, while the non–promising converge much faster.

Fig. 2 illustrates the convergence behavior. The swarm rapidly explores the design space during the first ~10 iterations, testing a wide range of capacities. After this phase, the search progressively focuses on exploitation, refining the best-performing configurations. Incremental improvements occur notably around iterations 11 and 22, associated with a reallocation between storage and electrolyzers. Interestingly, configurations with initially high RES and storage capacities (e.g., iteration 3) were eventually discarded, as they proved inefficient when evaluated against the specific demand profile and operational constraints of the proposed case study. This demonstrates that the integrated PSO–MILP framework effectively balances capacity expansion with operational feasibility.

5. Optimal water–energy planning: Results and discussion

This section presents the outcomes of the PSO–MILP optimization across all scenario configurations and water-demand multipliers. They are first summarized in Table 4, which reports the total annualized system cost (f_{obj}), RES share, fuel consumption, optimal planning configuration, and each technology's contribution to downward reserve provision. This comprehensive dataset provides the basis for a structured analysis of how reserve modeling assumptions, desalination dispatch optimization, and water demand intensity shape the techno-economic and operational characteristics of the energy–water system. In the following subsections, the discussion first examines how expanding the set of technologies eligible for downward reserve provision affects system costs, renewable penetration, and capacity allocation patterns. It then investigates the role of desalination as a flexible demand, comparing a fixed-load representation with a fully integrated co-optimization of its dispatch, and assessing the resulting changes in investment needs, operational costs, and flexibility provision. Finally, it explores the implications of increasing freshwater demand on energy system design, with particular attention to its impact on technology choices, fuel dependency, and storage utilization strategies.

5.1. Reserve modeling settings impact on energy planning

The results in Fig. 3 show a clear relationship between the reserve modeling approach and both economic and environmental performance. Allowing all technologies to provide reserves, rather than relying solely on diesel units, lowers the total objective cost by nearly 47%. Simultaneously, the renewable energy share in the generation mix increases from 41% to 87%, while fuel consumption falls to less than one-quarter of its original level. The increase in RES share from 41% to 87% is the combined effect of two mechanisms. Allowing multiple technologies (BESS, desalination, electrolyzers) to provide reserves increases the RES share from 41% to 85%, while enabling flexible desalination scheduling further raises it to 87%. These results highlight that enabling downward reserve provision from clean and flexible

Table 4
The results of the PSO-MILP water–energy planning optimization for all the scenarios considered.

Scenario		f_{obj}	RES	Fuel	Planning configuration (MW or MWh)						Reserve provision (MW)			
WD	Model setting	(M€/y)	Share (%)	(Ml)	PV	FOWT	BESS	DES	H2	ELY-FC	DGs	BESS	DES	ELY
×1	Reserve-DSL-Only	16	41	1202	15.0	1.00	30.5	0.75	97.5	1.07	1.96	12.06	0.01	0.84
	DES-NoOptDispatch	10	85	339	15.0	5.00	25.5	0.25	221	2.92	0.63	10.44	0.00	2.36
	FULL	9	87	269	15.0	6.00	23.5	0.75	229	3.08	0.50	9.96	0.00	2.43
×1.5	Reserve-DSL-Only	17	41	1209	15.0	1.00	31.5	1.50	150	1.50	1.98	12.67	0.04	1.24
	DES-NoOptDispatch	11	85	369	15.0	6.00	25.5	0.25	220.5	2.91	0.68	10.66	0.00	2.32
	FULL	10	83	339	15.0	6.00	23.0	1.50	156	1.62	0.63	9.85	0.02	1.25
×2	Reserve-DSL-Only	18	39	1255	15.0	2.00	29.0	2.00	57.5	1.15	2.06	12.11	0.04	0.89
	DES-NoOptDispatch	13	83	435	15.0	6.00	27.5	0.50	167.5	3.18	0.80	11.44	0.00	2.63
	FULL	10	81	372	15.0	7.00	22.0	1.50	150	3.00	0.69	9.60	0.00	2.37

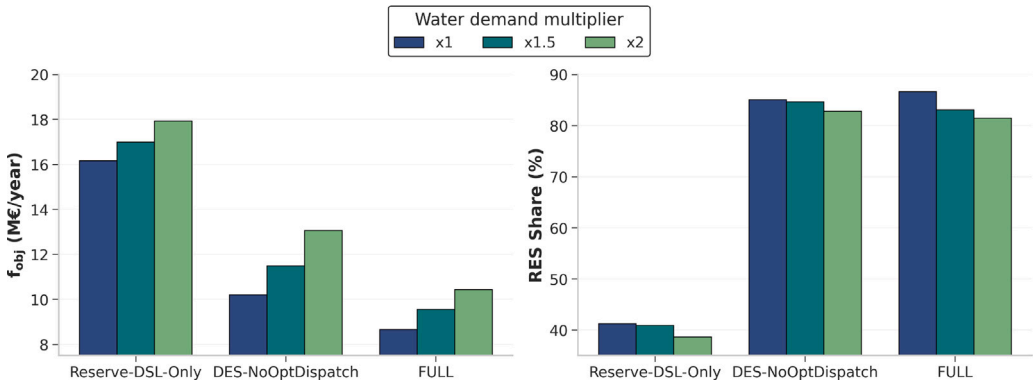

Fig. 3. f_{obj} and RES Share comparison with respect to scenarios.

technologies—primarily BESS, but also DES and ELY—significantly increases the economic attractiveness of installing vRES. By reducing the reliance on diesel units for system flexibility, the model identifies higher RES share as cost-effective, which in turn markedly lowers fuel dependency and associated operational costs.

5.2. Co-optimizing desalination dispatch as a flexible demand

In the DES-NoOptDispatch scenario, most of the freshwater demand is represented as an inelastic electrical load, meaning that DES operate independently of the power system's needs and renewable availability. The only component that remains time-varying is the share of water demand associated with H2 production, which continues to follow the operational profile of the ELY. This simplification decouples the bulk of desalination from system flexibility, forcing the installation of enough capacity to meet the peak freshwater demand regardless of the overall generation mix. In contrast, in the FULL configuration, desalination plants are co-optimized with the rest of the system, allowing their working hours to adapt to renewable generation patterns, storage availability, and reserve requirements. To provide an intuitive view of the resulting operational dynamics, Fig. 4 reports an illustrative 24-h average dispatch profile (hourly mean over the full year) for the FULL ×1 case, highlighting the interaction between vRES generation, flexible desalination, storage, and hydrogen pathways.

This flexibility substantially increases their contribution to system cost-effectiveness: based on Fig. 3, optimizing desalination dispatch yields cost savings of around 15% for WD multipliers of ×1 and ×1.5, and up to 30% for ×2. The relative benefit grows with higher freshwater demand, as the economic penalty of oversizing non-optimized desalination capacity becomes increasingly significant.

This trend is further confirmed by Fig. 5, which illustrates the dispatch strategy adopted to operate DES across the entire time horizon. When demand-side management is enabled, the optimal strategy consists of aggregating water demand into fewer operating periods—always within the imposed technical constraints of minimum up-time and minimum load—thus ensuring proper system functioning. The strong discrepancy between the two scenarios, reflected in the different operating costs driven by standby expenditures, highlights the importance of co-optimizing the operational strategy of both the water and energy layers within a unified framework.

5.3. Water scarcity and energy planning interaction

An increase in freshwater demand directly translates into higher electricity consumption. While in principle this additional demand could be met by a proportional rise in renewable generation, the results instead show a reduction of a few percentage points in RES share, with a corresponding increase in diesel generation. Given that PV capacity is already saturated in all scenarios starting from ×1, its output naturally cannot grow—and indeed remains unchanged—but this is expected. As shown in Fig. 6, the more relevant observation lies in the behavior of other technologies: FOWT does not increase, except in the most extreme case (×2), where it rises by approximately 17% (from 6 to 7 MW), a modest change compared to the substantial growth in total electricity demand of 6 MWh per year. This suggests that the optimizer tends to preserve the existing technology mix rather than expand FOWT, likely due to its higher marginal cost and lower synergy with the residual demand profile.

Equally noteworthy is the fact that storage technologies—both BESS and H2-based—do not expand under higher water demand, and in some cases their installed capacity even decreases. This counterintuitive result stems from the fact that, as freshwater demand grows, the ability to adjust desalination operation to absorb excess renewable production becomes even more valuable, reducing the relative need for additional energy storage. Indeed, when desalination operability is fully optimized, DES effectively acts as a "virtual storage" resource with negligible marginal cost for absorbing RES peaks, directly competing with BESS and ELY in providing system flexibility and thereby lowering the incentive to invest in additional storage capacity. Consequently,

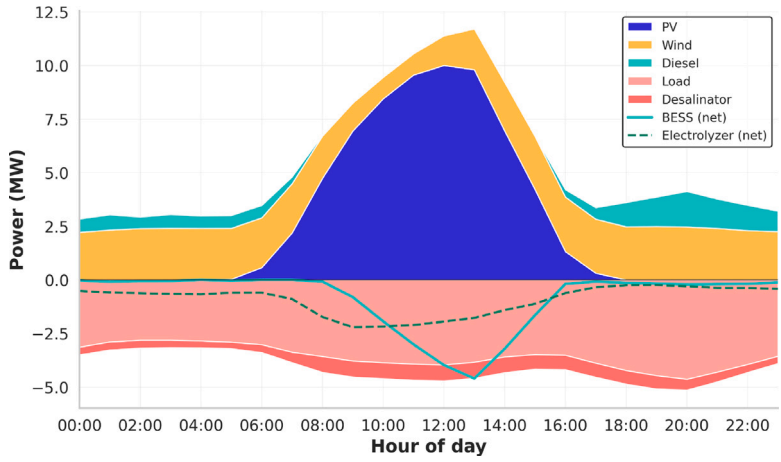

Fig. 4. 24-hour average power (hourly mean over the full year) for the FULL×1 case.

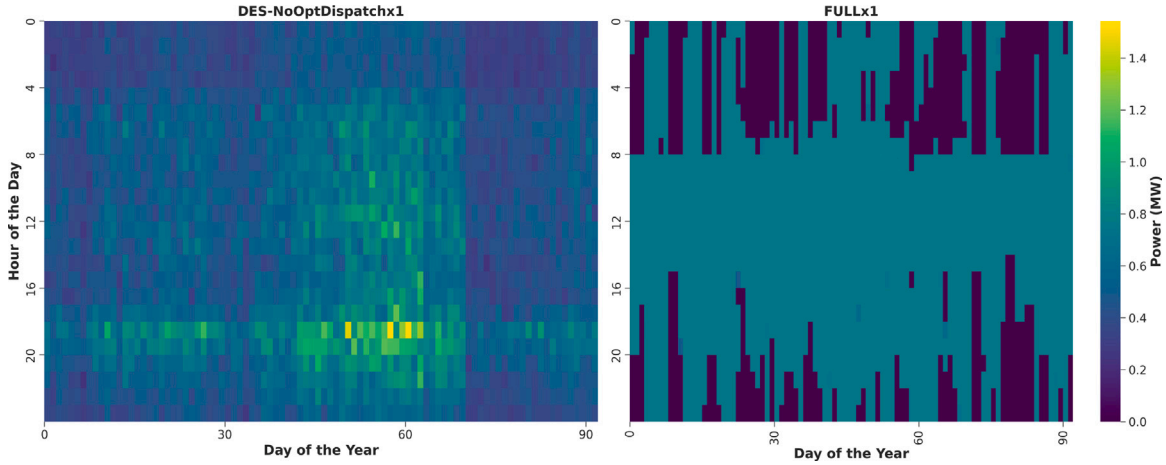

Fig. 5. Dispatched power profile of desalination units for DES-NoOptDispatchx1 and FULLx1 scenarios.

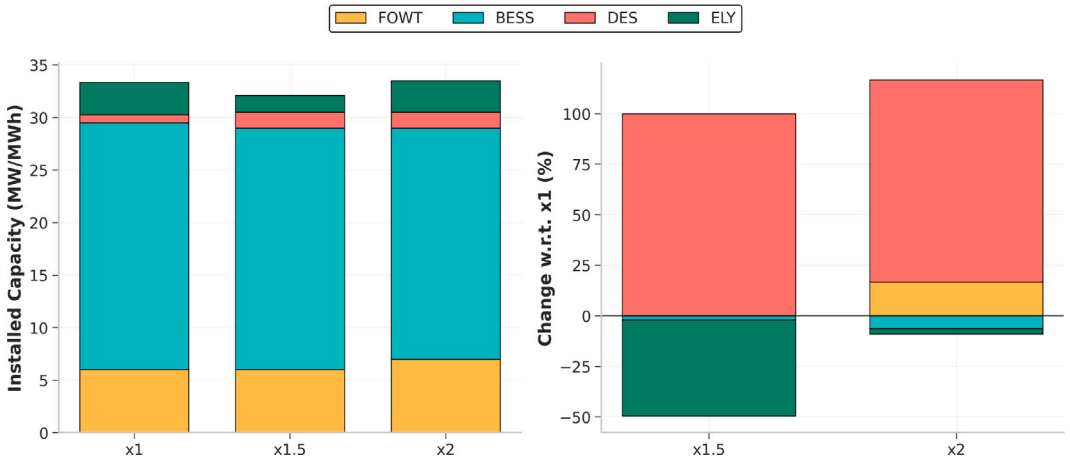

Fig. 6. Installed capacities and relative variations for different demand multipliers under the FULLx1 scenario.

the integrated optimization of water and energy systems becomes increasingly critical in high-demand scenarios, as it allows desalination to operate as a strategic flexibility provider that mitigates curtailment, supports renewable integration, and reduces overall system costs.

6. Conclusions

This paper has presented a novel PSO-MILP optimization framework for integrated water–energy planning, designed to capture the tight interdependencies between desalination, hydrogen production, and power system operation under reserve requirements. The framework addresses the limitations of existing models by simultaneously incorporating long-term planning and short-term operational constraints, thereby offering a more realistic representation of small isolated systems exposed to both water scarcity and high RES potential.

Its application to Pantelleria provides a concrete and policy-relevant case, as the island currently relies entirely on diesel generation while facing structural water shortages and untapped renewable potential. The results highlight how flexible desalination scheduling and reserve co-optimization can transform water demand from a burden into a source of system flexibility, effectively acting as virtual storage.

Quantitatively, enabling reserve provision beyond diesel units to clean technologies such as BESS lowers total system costs by nearly 47% and raises the renewable share from 41% to 87%. Optimizing desalination dispatch further reduces fuel reliance and operational expenditures, yielding up to 30% cost savings compared to a fixed-load representation. Finally, when freshwater demand doubles, the renewable share declines by only 6%, with FOWT capacity rising by just 17%, confirming that the system maintains high flexibility through demand-side coordination rather than additional storage or generation.

The quantitative results presented in this work are contingent on the adopted downward reserve formulation and associated parameters (i.e. water tank size). While this formulation is consistent and robust for the analyzed case study, different reserve definitions or operator practices may lead to different quantitative outcomes. This aspect, combined with grid stability assessments, represents an important direction for future extensions of the framework.

Overall, these findings demonstrate the value of integrating water and energy planning in small island systems, not only for improving cost-effectiveness and decarbonization, but also for ensuring resilience under increasing water demand.

CRediT authorship contribution statement

Matteo Savina: Writing – original draft, Software, Methodology, Investigation, Data curation. **Carlo Federico Vescovo:** Software, Investigation, Data curation. **Giovanni Zaccaria:** Writing – original draft, Software, Investigation, Data curation. **Enrico Giglio:** Writing – review & editing, Writing – original draft, Supervision, Methodology, Conceptualization. **Giuliana Mattiazzo:** Project administration, Funding acquisition.

Declaration of competing interest

The authors declare that they have no known competing financial interests or personal relationships that could have appeared to influence the work reported in this paper.

Acknowledgments & funding

The Project is funded under the National Recovery and Resilience Plan (NRRP), Italy, Mission 4 Component 2 Investment 1.3 - Call for tender No. 1561 of 11.10.2022 of Ministero dell'Università e della Ricerca (MUR); funded by the European Union – NextGenerationEU Award Number: Project code PE0000021, Concession Decree No. 1561 of 11.10.2022 adopted by Ministero dell'Università e della Ricerca (MUR), Italy, CUP, Italy E13C22001890001, Project title "Network 4 Energy Sustainable Transition – NEST".

Data availability

Data will be made available on request.

References

Abdelsalam, R.A., Farag, H., Zeineldin, H., El-saadany, E., 2024. Optimal energy management system for green hydrogen production and seawater desalination plants with demand response integration. In: 2024 IEEE Industrial Electronics and Applications Conference (IEACon). IEEE, pp. 136–140.

Abdi, H., Ranjbaran, M., Nazari, P., Akbari, H., 2013. A review on pso models in power system operation. Int. J. Emerg. Technol. Adv. Eng. 3 (7).

Airoldi, D., Bertani, D., Garofalo, E., Guastella, S., Lembo, E., Sandroni, C., Giudici, F., 2017. Scenari Di Sviluppo Delle FER Nelle Isole Minori Italiane Non Interconnesse E Analisi Di Casi Studio. Tech. Rep. Rapporto 17004171, Ricerca sul Sistema Energetico – RSE S.p.A., Milano, Italy, Deliverable n.14, as part of the Accordo di programma 2015-2017 with the Italian Ministry of Economic Development.

Al-Mubarak, M.J., Conejo, A.J., 2025. Expansion planning via decomposition to achieve fully renewable power and freshwater systems. Sustain. Energy Grids Netw. (101713), 101713.

Almasoudi, S., Jamoussi, B., 2024. Desalination technologies and their environmental impacts: A review. Sustain. Chem. One World 1, 100002. http://dx.doi.org/10.1016/j.scowo.2024.100002, URL https://www.sciencedirect.com/science/article/pii/S2950357424000027.

Alnahhal, Z., Shaaban, M.F., Hamouda, M.A., Majozi, T., Bardan, M.A., 2023. A water-energy nexus approach for the co-optimization of electric and water systems. IEEE Access 11, 28762–28770.

Arunachalam, M., Yoo, Y., Al-Ghamdi, A.S., Park, H., Han, D.S., 2024. Integrating green hydrogen production with renewable energy-powered desalination: An analysis of CAPEX implications and operational strategies. Int. J. Hydrog. Energy 84, 344–355.

Astolfi, M., Mazzola, S., Silva, P., Macchi, E., 2017. A synergic integration of desalination and solar energy systems in stand-alone microgrids. Desalination 419, 169–180.

Babatunde, O., Munda, J., Hamam, Y., 2020. Power system flexibility: A review. Energy Rep. 6, 101–106. http://dx.doi.org/10.1016/j.egyr.2019.11.048, The 6th International Conference on Power and Energy Systems Engineering. URL https://www.sciencedirect.com/science/article/pii/S2352484719309242.

Blechinger, P., Cader, C., Bertheau, P., Huyskens, H., Seguin, R., Breyer, C., 2016. Global analysis of the techno-economic potential of renewable energy hybrid systems on small islands. Energy Policy 98, 674–687. http://dx.doi.org/10.1016/j.enpol.2016.03.043, URL https://www.sciencedirect.com/science/article/pii/S0301421516301471.

Brijs, T., van Stiphout, A., Siddiqui, S., Belmans, R., 2017. Evaluating the role of electricity storage by considering short-term operation in long-term planning. Sustain. Energy, Grids Networks 10, 104–117. http://dx.doi.org/10.1016/j.segan.2017.04.002, URL https://www.sciencedirect.com/science/article/pii/S2352467716301102.

Brown, T., Hörsch, J., Schlachtberger, D., 2018. PyPSA: Python for Power System Analysis. J. Open Res. Softw. 6 (4), http://dx.doi.org/10.5334/jors.188, arXiv:1707.09913.

Corsini, A., Rispoli, F., Gamberale, M., Tortora, E., 2009. Assessment of H2-and H2O-based renewable energy-buffering systems in minor islands. Renew. Energy 34 (1), 279–288.

EL-Qasery, M., Abbou, A., Laamim, M., Id-Khajine, L., Rochd, A., 2025. Comparative analysis of GA and PSO algorithms for optimal cost management in on-grid microgrid energy systems with PV-battery integration. Glob. Energy Interconnect. 8 (4), 572–580. http://dx.doi.org/10.1016/j.gloei.2025.05.003.

Elbalki, M., Shaaban, M.F., Osman, A., Pietrasanta, A., Kamil, M., Ali, A., 2024. Optimizing integrated water and electrical networks through a holistic water–energy nexus approach. Sustainability 16 (9), 3783.

Elsir, M., Al-Awami, A.T., Antar, M.A., Oikonomou, K., Parvania, M., 2022. Risk-based operation coordination of water desalination and renewable-rich power systems. IEEE Trans. Power Syst. 38 (2), 1162–1175.

Esmaeilion, F., Soltani, M., Luna-Triguero, A., 2025. Soft computing optimization of a renewable energy-integrated multigeneration system with liquid air energy storage. J. Energy Storage 127 (117140), 117140.

Esquivel-Puentes, H.A., Vacca, A., Chamorro, L.P., Garcia-Bravo, J., Warsinger, D.M., Castillo, L., 2025. Simultaneous electricity generation and low-energy-intensive water desalination using a hydraulic wind turbine. Desalination 601, 118526. http://dx.doi.org/10.1016/j.desal.2025.118526, URL https://www.sciencedirect.com/science/article/pii/S0011916425000013.

Gad, A.G., 2022. Particle swarm optimization algorithm and its applications: A systematic review. Arch. Comput. Methods Eng. 29 (5), 2531–2561. http://dx.doi.org/10.1007/s11831-021-09694-4.

Giglio, E., Carà, C., Pasta, E., Destro, E., Ceni, A., Bracco, G., Mattiazzo, G., 2025a. An integrated MILP framework for co-optimizing energy and water systems with up and downward reserve constraints: Application to an off-grid small island. Appl. Energy 401, 126821. http://dx.doi.org/10.1016/j.apenergy.2025.126821, URL https://www.sciencedirect.com/science/article/pii/S030626192501551X.

Giglio, E., Fioriti, D., Chihota, M.J., Poli, D., Bekker, B., Mattiazzo, G., 2025b. Integrated stochastic reserve estimation and MILP energy planning for high renewable penetration: Application to 2050 South African energy system. Sustain. Energy, Grids Networks 42, 101650. http://dx.doi.org/10.1016/j.segan.2025.101650, URL https://www.sciencedirect.com/science/article/pii/S2352467725000323.

Giglio, E., Novo, R., Mattiazzo, G., Fioriti, D., 2023. Reserve provision in the optimal planning of off-grid power systems: Impact of storage and renewable energy. IEEE Access 11, 100781–100797.

Giglio, E., Pasta, E., Poli, D., Mattiazzo, G., Fioriti, D., 2025c. Capacity expansion and unit commitment with reserve requirements: A comparative analysis for an Italian off-grid island. In: 2025 21st International Conference on the European Energy Market. EEM, pp. 1–7. http://dx.doi.org/10.1109/EEM64765.2025.11050131.

Giglio, E., Savina, M., Vescovo, C.F., Zaccaria, G., 2025d. Pso-milp-water-energy. https://github.com/pso-energy/pso-milp-water-energy,

Giorcelli, F., Giglio, E., Sirigu, S.A., Mattiazzo, G., 2025. Power grid informed techno-economic analysis of the optimal pewec design. Energy 334, 137708. http://dx.doi.org/10.1016/j.energy.2025.137708, URL https://www.sciencedirect.com/science/article/pii/S036054422503350X.

Go, J., Byun, J., Orehounig, K., Heo, Y., 2023. Battery-H2 storage system for self-sufficiency in residential buildings under different electric heating system scenarios. Appl. Energy 337, 120742. http://dx.doi.org/10.1016/j.apenergy.2023.120742, URL https://www.sciencedirect.com/science/article/pii/S030626192300106X.

Groppi, D., Feijoo, F., Pfeifer, A., Garcia, D.A., Duic, N., 2023. Analyzing the impact of demand response and reserves in islands energy planning. Energy 278, 127716.

Grubert, E., 2023. Water consumption from electrolytic hydrogen in a carbon-neutral US energy system. Clean. Prod. Lett. 4, 100037. http://dx.doi.org/10.1016/j.clpl.2023.100037, URL https://www.sciencedirect.com/science/article/pii/S2666791623000106.

Guo, Q., Guo, T., Tian, Q., Nojavan, S., 2021. Optimal robust scheduling of energy-water nexus system using robust optimization technique. http://dx.doi.org/10.1016/j.compchemeng.2021.107542.

Helerea, E., Calin, M.D., Musuroi, C., 2023. Water energy nexus and energy transition—A review. Energies 16 (4), http://dx.doi.org/10.3390/en16041879, URL https://www.mdpi.com/1996-1073/16/4/1879.

Hersbach, H., Bell, B., Berrisford, P., Hirahara, S., Horányi, A., Muñoz-Sabater, J., Nicolas, J., Peubey, C., Radu, R., Schepers, D., Simmons, A., Soci, C., Abdalla, S., Abellan, X., Balsamo, G., Bechtold, P., Biavati, G., Bidlot, J., Bonavita, M., De Chiara, G., Dahlgren, P., Dee, D., Diamantakis, M., Dragani, R., Flemming, J., Forbes, R., Fuentes, M., Geer, A., Haimberger, L., Healy, S., Hogan, R.J., Hólm, E., Janisková, M., Keeley, S., Laloyaux, P., Lopez, P., Lupu, C., Radnoti, G., de Rosnay, P., Rozum, I., Vamborg, F., Villaume, S., Thépaut, J.-N., 2020. The ERA5 global reanalysis. Q. J. R. Meteorol. Soc. 146 (730), 1999–2049. http://dx.doi.org/10.1002/qj.3803, arXiv:https://rmets.onlinelibrary.wiley.com/doi/pdf/10.1002/qj.3803 URL https://rmets.onlinelibrary.wiley.com/doi/abs/10.1002/qj.3803.

Jain, M., Saihjpal, V., Singh, N., Singh, S.B., 2022. An overview of variants and advancements of PSO algorithm. Appl. Sci. 12 (17), 8392.

Kaldellis, J., Tzanes, G., Papapostolou, C., Kavadias, K., Zafirakis, D., 2017. Analyzing the limitations of vast wind energy contribution in remote island networks of the aegean sea archipelagos. Energy Procedia 142, 787–792. http://dx.doi.org/10.1016/j.egypro.2017.12.127, Proceedings of the 9th International Conference on Applied Energy. URL https://www.sciencedirect.com/science/article/pii/S1876610217358551.

Kennedy, J., Eberhart, R., 1995. Particle swarm optimization. In: Proceedings of ICNN'95 - International Conference on Neural Networks, vol. 4, pp. 1942–1948 vol.4. http://dx.doi.org/10.1109/ICNN.1995.488968.

Liu, B., Rahimpour, H., Musleh, A.S., Zhang, D., Thattai, K., Dong, Z.Y., 2023. Multi-objective optimal day-ahead scheduling of desalination-hydrogen system powered by hybrid renewable energy sources. J. Clean. Prod. 414, 137737. http://dx.doi.org/10.1016/j.jclepro.2023.137737, URL https://www.sciencedirect.com/science/article/pii/S0959652623018954.

Mehrjerdi, H., 2020a. Modeling and integration of water desalination units in thermal unit commitment considering energy and water storage. Desalination 483, 114411. http://dx.doi.org/10.1016/j.desal.2020.114411, URL https://www.sciencedirect.com/science/article/pii/S0011916419323823.

Mehrjerdi, H., 2020b. Modeling and optimization of an island water-energy nexus powered by a hybrid solar-wind renewable system. Energy 197, 117217. http://dx.doi.org/10.1016/j.energy.2020.117217, URL https://www.sciencedirect.com/science/article/pii/S0360544220303248.

Mentis, D., Karalis, G., Zervos, A., Howells, M., Taliotis, C., Bazilian, M., Rogner, H., 2016. Desalination using renewable energy sources on the arid islands of south aegean sea. Energy 94, 262–272.

Meschede, H., Bertheau, P., Khalili, S., Breyer, C., 2022. A review of 100% renewable energy scenarios on islands. WIREs Energy Environ. 11 (6), e450. http://dx.doi.org/10.1002/wene.450, URL https://wires.onlinelibrary.wiley.com/doi/abs/10.1002/wene.450.

Mohammadi, F., Sahraei-Ardakani, M., Al-Abdullah, Y., Heydt, G.T., 2019. Can desalination be an economically viable solution for water scarcity? In: 2019 IEEE Global Humanitarian Technology Conference. GHTC, pp. 1–4. http://dx.doi.org/10.1109/GHTC46095.2019.9033050.

Moscoloni, C., Zarra, F., Novo, R., Giglio, E., Vargiu, A., Mutani, G., Bracco, G., Mattiazzo, G., 2022. Wind turbines and rooftop photovoltaic technical potential assessment: Application to sicilian minor islands. Energies 15 (15), http://dx.doi.org/10.3390/en15155548, URL https://www.mdpi.com/1996-1073/15/15/5548.

Oikonomou, K., Parvania, M., 2019. Optimal participation of water desalination plants in electricity demand response and regulation markets. IEEE Syst. J. 14 (3), 3729–3739.

Palmeros Parada, M., Randazzo, S., Gamboa, G., Ktori, R., Bouchaut, B., Cipolina, A., Micale, G., Xevgenos, D., 2023. Resource recovery from desalination, the case of small islands. Resour. Conserv. Recycl. 199, 107287. http://dx.doi.org/10.1016/j.resconrec.2023.107287, URL https://www.sciencedirect.com/science/article/pii/S0921344923004214.

Rosa, L., Sangiorgio, M., 2025. Global water gaps under future warming levels. Nat. Commun. 16 (1), 1192.

Segurado, R., Krajačić, G., Duić, N., Alves, L., 2011. Increasing the penetration of renewable energy resources in s. Vicente, cape verde. Appl. Energy 88 (2), 466–472.

Simoes, S.G., Catarino, J., Picado, A., Lopes, T.F., di Berardino, S., Amorim, F., Gírio, F., Rangel, C., Ponce de Leão, T., 2021. Water availability and water usage solutions for electrolysis in hydrogen production. J. Clean. Prod. 315, 128124. http://dx.doi.org/10.1016/j.jclepro.2021.128124, URL https://www.sciencedirect.com/science/article/pii/S0959652621023428.

Stunjek, G., Krajačić, G., 2025. Optimisation of desalination-based water system with integrated renewable energy and storage within the water-energy nexus. Desalination 600 (118474), 118474.

Vakilifard, N., Anda, M., A. Bahri, P., Ho, G., 2018. The role of water-energy nexus in optimising water supply systems – review of techniques and approaches. Renew. Sustain. Energy Rev. 82, 1424–1432. http://dx.doi.org/10.1016/j.rser.2017.05.125, URL https://www.sciencedirect.com/science/article/pii/S1364032117307621.

Wen, D., Kuo, P.-C., Aziz, M., 2024. Novel renewable seawater desalination system using hydrogen as energy carrier for self-sustaining community. Desalination 579 (117475), 117475.

Zein, A., Karaki, S., Al-Hindi, M., 2023. Analysis of variable reverse osmosis operation powered by solar energy. Renew. Energy 208, 385–398. http://dx.doi.org/10.1016/j.renene.2023.03.001, URL https://www.sciencedirect.com/science/article/pii/S0960148123002872.